Reduction of dilute Ising spin glasses

Stefan Boettcher* and James Davidheiser†
Physics Department, Emory University, Atlanta, Georgia 30322, USA
(Received 19 March 2008; revised manuscript received 24 May 2008; published 25 June 2008)

The recently proposed reduction method for diluted spin glasses is investigated in depth. In particular, the Edwards-Anderson model with $\pm J$ and Gaussian bond disorder on hypercubic lattices in $d=2$, 3, and 4 is studied for a range of bond dilutions. The results demonstrate the effectiveness of using bond dilution to elucidate low-temperature properties of Ising spin glasses and provide a starting point to enhance the methods used in reduction. Based on that, a greedy heuristic called "dominant bond reduction" is introduced and explored.

DOI: 10.1103/PhysRevB.77.214432 PACS number(s): 02.60.Pn, 05.50.+q, 75.10.Nr

I. INTRODUCTION

Despite more than three decades of intensive research, many properties of spin glasses,[1–4] especially in finite dimensions, are still not well understood. The simplest model is the Edwards-Anderson (EA) model,[5]

$$H = -\sum_{\langle i,j\rangle} J_{i,j} x_i x_j, \quad (x_i = \pm 1), \tag{1}$$

with Ising spins $x_i = \pm 1$ arranged on a finite-dimensional lattice with nearest-neighbor bonds $J_{i,j}$, randomly drawn from a distribution $P(J)$ of zero mean and unit variance.

In Refs. 6–8, it was proposed to study the EA in Eq. (1) on bond-diluted lattices at $T=0$ to obtain more accurate scaling behavior for low-temperature excitations. There, it is shown how to remove iteratively low-connected spins from the lattice and alter the interactions, i.e., to *reduce* the system, in such a way that the ground-state energy of the reduced system is the same as the original system. In this way often much larger lattice sizes L can be simulated compared to undiluted ones and, in combination with finite-size scaling, enhanced scaling regimes are achieved. With these methods, for instance, we have solved spin glasses exactly at the bond-percolation threshold p_c, the edge of the glassy regime, in $d=2,\ldots,7$ by reducing a large number of systems with up to 10^8 spins.[9]

There is, of course, a long history of studying spin systems on dilute lattices, including spin glasses, going back to Ref. 5 itself (see, for example, Refs. 10–14). Coniglio[15,16] proposed to map the ensemble of critical Ising (or Potts) spin models onto percolating clusters, based on the ideas of Fortuin and Kasteleyn,[17] to treat ferromagnetic[18] and spin-glass phenomena.[19,20] Our approach here is based on transformations in the Hamiltonian of an Ising spin system that are *exact* for each instance. The price paid is that these transformations reducing the Hamiltonian only apply at $T=0$. Extending our earlier work on the Migdal-Kadanoff approximation,[8] Jörg and Ricci-Tersenghi[21] very recently included infinitesimal temperature corrections. Their method is limited to discrete bonds and to a subset of the rules we discuss here. As we can merely consider $T=0$, we are unfortunately not sensitive to the transition seen by Ref. 21 that is said to emerge only at nonzero temperatures.

Our approach, combined with the highly efficient "extremal optimization" (EO) heuristic,[22,23] have lead to a comprehensive characterization of low-temperature excitations in spin glasses in low dimensions (up to $d=7$).[24] These results allow for a direct comparison with mean-field predictions[25] and have recently motivated a reassessment of fundamental scaling relations.[26,27] This work has also inspired the use of dilution for more effective Monte Carlo simulations of disordered systems.[21,28–30]

Here we study the connection between lattice topology and the reduction method. In particular, we explore the effectiveness of each of the reduction rules as a function of bond dilution. The results provide the reader with an opportunity to evaluate in more detail the conclusions drawn in previous papers[6,7,24,31,32] and might suggest possible extensions of these rules for improved effectiveness. As an example of a concrete application, we introduce and evaluate "dominant bond reduction" (DBR), a new heuristic which entails a greedy, almost linear algorithm to obtain approximate spin-glass ground states on average with bounded relative error for increasing system sizes.

This paper is structured as follows. In Sec. II, we will introduce the reduction method and its rules. In Sec. III, we display and discuss our numerical investigation of the reduction rules. In Sec. VI, we discuss our simulation results for DBR, followed by some concluding remarks in Sec. V. In the Appendix, a generalized description of the reduction method is given with some speculations on its applicability.

II. REDUCTION METHOD

To exploit the advantages of spin glasses on a bond-diluted lattice, we can often *reduce* the number of relevant degrees of freedom substantially before a call to an optimization algorithm becomes necessary. Such a reduction, in particular, of low-connected spins, leads to a smaller compact remainder graph, bare of trivially fluctuating variables, which is easier to optimize. These reductions are very similar to a procedure known as k-core decomposition in graph theory, which is often applied to analyze hard combinatorial or real-world problems.[33–35] Furthermore, rules of this sort have also been used to study planar[36] and $3d$ resistor networks.[37]

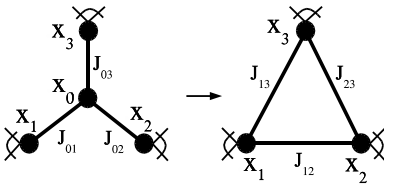

FIG. 1. "Star-triangle" relation to reduce a three-connected spin x_0. The new bonds on the right are obtained in Eq. (4).

Here, we focus exclusively on the reduction rules for the ground-state energy (i.e., $T=0$); a subset of these rules also permits the exact determination of the entropy and overlap[8] at $T=0$. These rules apply to general Ising spin-glass Hamiltonians as in Eq. (1) with *any* bond distribution $P(J)$, discrete or continuous, on arbitrary sparse graphs.

The reductions affect both spins and bonds, eliminating recursively all zero-, one-, two-, and three-connected spins. These rules are supplemented here with one that is not topological but concerns bond values directly, which is especially effective for broad continuous bond distributions, such as Gaussian or power-law bonds. The addition of more elaborate rules that depend on suitably chosen bond distributions is conceivable, the universality of the underlying physics permitting. These operations eliminate and add terms to the expression for the Hamiltonian in Eq. (1) but leave it *form invariant*. Again, loosening this requirement may lead to an even more efficient procedure for certain problems, although it should be understood that an unrestricted reduction in general leads to an exponential growth in the number and form of the newly created terms, involving all combinations of p-spin interactions (see the Appendix). Offsets in the energy along the way are accounted for by a variable H_o, which is *exact* for a ground-state configuration. The rules discussed here are as follows:

Rule I: An isolated spin can be ignored entirely.

Rule II: A one-connected spin i can be eliminated since its state can always be chosen in accordance with its neighboring spin j to satisfy the bond $J_{i,j}$. For its energetically most favorable state, we adjust $H_o := H_o - |J_{i,j}|$ and eliminate the term $-J_{i,j}x_i x_j$ from H.

Rule III: A double bond, $J_{i,j}^{(1)}$ and $J_{i,j}^{(2)}$, between two spins i and j can be combined to a single bond by setting $J_{i,j}=J_{i,j}^{(1)}+J_{i,j}^{(2)}$ or be eliminated entirely if the resulting bond vanishes. This operation is very useful to lower the connectivity of i and j at least by one (for example, see Fig. 2).

Rule IV: For a two-connected spin i, rewrite the two terms pertaining to x_i in Eq. (1) as

$$x_i(J_{i,1}x_1 + J_{i,2}x_2) \leq |J_{i,1}x_1 + J_{i,2}x_2| = J_{1,2}x_1x_2 + \Delta H, \quad (2)$$

where

$$J_{1,2} = \frac{1}{2}(|J_{i,1} + J_{i,2}| - |J_{i,1} - J_{i,2}|),$$

$$\Delta H = \frac{1}{2}(|J_{i,1} + J_{i,2}| + |J_{i,1} - J_{i,2}|), \quad (3)$$

leaving the graph with a new bond $J_{1,2}$ between spins 1 and 2 and acquiring an offset $H_o := H_o - \Delta H$. In the ground state, the bound in Eq. (2) becomes an equality.

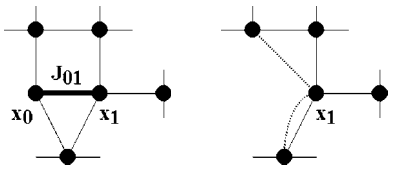

FIG. 2. Illustration of rule VI for "strong" bonds. Left: the local topology of a graph is shown for two spins, x_0 and x_1, connected by a bond $J_{0,1}$ (thick line). If $J_{0,1}>0$ ($J_{0,1}<0$) satisfies Eq. (5), x_0 and x_1 must align (antialign) in the ground state and x_0 can be removed. Right: the remainder graph is shown after the removal. The other bonds emanating from x_0 (dashed lines) are now directly connected to x_1 (with a sign change if $J_{0,1}<0$). This procedure may lead to a double bond (rule III), as shown here, if x_1 was already connected to a neighbor of x_0 before.

Rule V: A three-connected spin i can be reduced via a "star-triangle" relation, as depicted in Fig. 1. We rewrite the three terms pertaining to x_i in Eq. (1) as

$$\begin{aligned} J_{i,1}x_i x_1 + J_{i,2}x_i x_2 + J_{i,3}x_i x_3 &\leq |J_{i,1}x_1 + J_{i,2}x_2 + J_{i,3}x_3| \\ &= J_{1,2}x_1x_2 + J_{1,3}x_1x_3 + J_{2,3}x_2x_3 \\ &\quad + \Delta H, \end{aligned} \quad (4)$$

where

$$J_{1,2} = -A - B + C + D, \quad J_{1,3} = A - B + C - D,$$

$$J_{2,3} = -A + B + C - D, \quad \Delta H = A + B + C + D,$$

$$A = \frac{1}{4}|J_{i,1} - J_{i,2} + J_{i,3}|, \quad B = \frac{1}{4}|J_{i,1} - J_{i,2} - J_{i,3}|,$$

$$C = \frac{1}{4}|J_{i,1} + J_{i,2} + J_{i,3}|, \quad D = \frac{1}{4}|J_{i,1} + J_{i,2} - J_{i,3}|.$$

As before, in the ground state, the bound in Eq. (4) becomes an equality.

Rule VI: A spin i (of any connectivity) for which the absolute weight $|J_{i,j'}|$ of one bond to a spin j' is larger than the absolute sum of all its other bond weights to neighboring spins $j \neq j'$, i.e.,

$$|J_{i,j'}| > \sum_{j \neq j} |J_{i,j}|, \quad (5)$$

bond $J_{i,j'}$ *must* be satisfied in any ground state. Then, spin i is determined in the ground state by spin j' and it, as well as this "superbond" $J_{i,j'}$, can be eliminated accordingly, as depicted in Fig. 2. Here, we obtain $H_0 := H_0 - |J_{i,j'}|$. All other bonds connected to i are simply reconnected with j', but with reversed sign, if $J_{i,j'}<0$.

This procedure is costly, and hence best applied after the other rules are exhausted. However, it can be highly effective for very widely distributed bonds. In particular, since neighboring spins may reduce in connectivity and become susceptible to the previous rules again, an avalanche of further reductions may ensue (see Fig. 2).

After a recursive application of these rules, the original lattice or graph is either completely reduced (which is almost

TABLE I. List of the range of system sizes L chosen for each dimension d in Figs. 3–6.

d	L
2	10, 20, . . . , 100
3	5, 10, . . . , 20
4	3, 4, . . . , 10, 15

always the case below or near p_c), in which case H_o provides the exact ground-state energy already, or we are left with a reduced, compact graph in which no spin has less than four connections, from which one could obtain the ground state with some optimization procedure, as described in Refs. 6 and 31. Reducing even higher-connected spins would lead to new (hyper)bonds between more than two spins, unlike Eq. (1), as discussed in the Appendix.

III. NUMERICAL SIMULATIONS

In our simulations we have studied EA spin glasses on hypercubic lattices over a range of sizes L in dimensions $d=2$, 3, and 4 at various bond fractions p for $\pm J$ bonds and Gaussian bonds. Similar studies could as well have been done on an arbitrary family of sparse graphs, without restriction. We have applied the rules described in Sec. II recursively, until no further reductions were possible. We have calculated a number of aspects of this reduction, such as the number of spins in the remainder graph relative to the original lattice, the average connectivity in the remainder graph, and the fraction of systems that is completely reducible (without remainder), all as a function of bond density p. Similarly, we have counted along the way how many times each of the reduction rules has been applied for graphs of a certain size L and bond fraction p. The system sizes used in each figure of this section are listed in Table I for each dimension.

In Fig. 3 we have plotted the efficiency of the reduction step for one-connected spins (rule II above, labeled R1 here), two-connected spins (rule IV, R2 here), three-connected spins (rule V, R3), double bond elimination (rule III, Rd), and superbonds (rule VI, SB) as a function of p for dimensions $d=2$, 3, and 4. Efficiency is defined here as the number of calls to that step in a run relative to the original number of spins $N=L^d$ in the lattice. We observe that each of the reduction rules reaches a peak for increasing bond densities, on order of R1, R2, R3, and SB. Rd, the elimination of double bonds, actually does not itself involve the reduction of a spin, and its behavior is more varied. The rise to that peak is

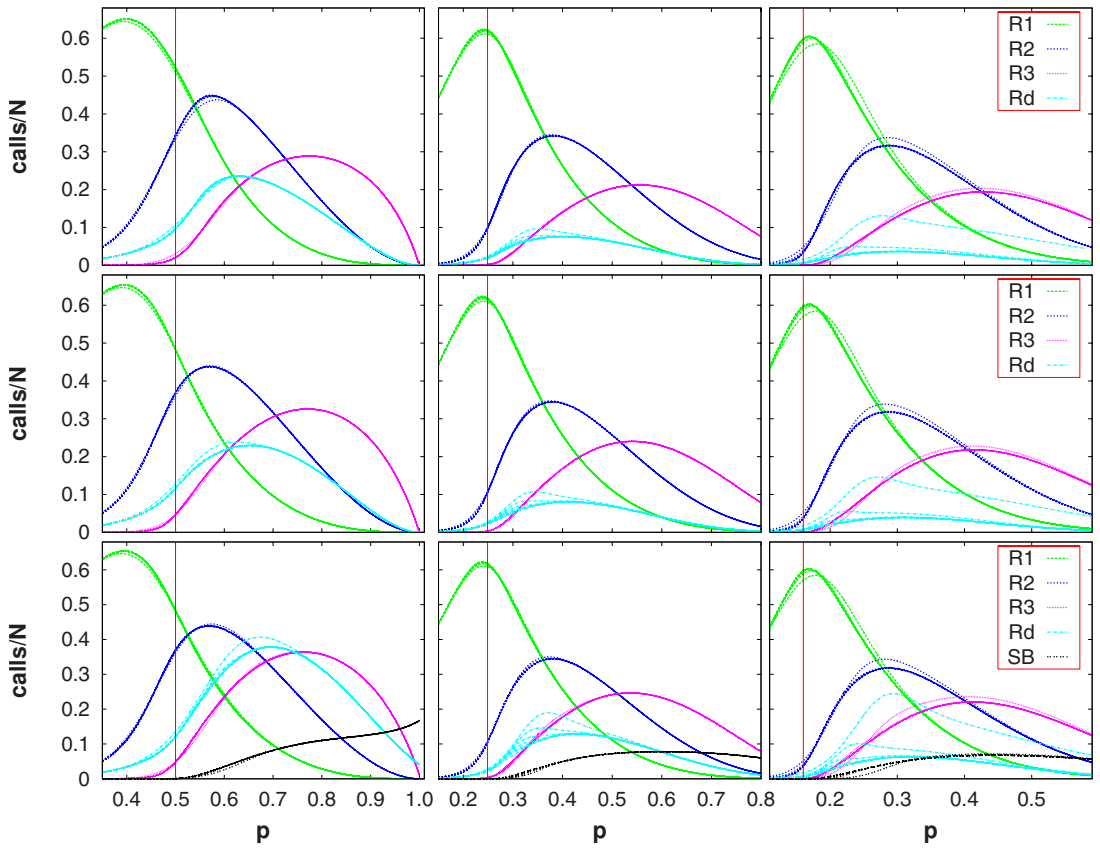

FIG. 3. (Color online) Plot of the efficiency of the reduction steps as a function of bond density p in $d=2$ (left column), $d=3$ (middle column), and $d=4$ (right column) for $\pm J$ bonds (top row), Gaussian bonds without superbond reduction SB according to rule VI (middle row), and Gaussian bonds with SB (bottom row). All efficiencies quickly become independent of system size L with closer-spaced curves corresponding to larger sizes. Rule VI, which is useful only for continuous bonds, does not effect other rules much but adds up to 10% in reduction even at $p=1$ with decreasing effect for larger d.

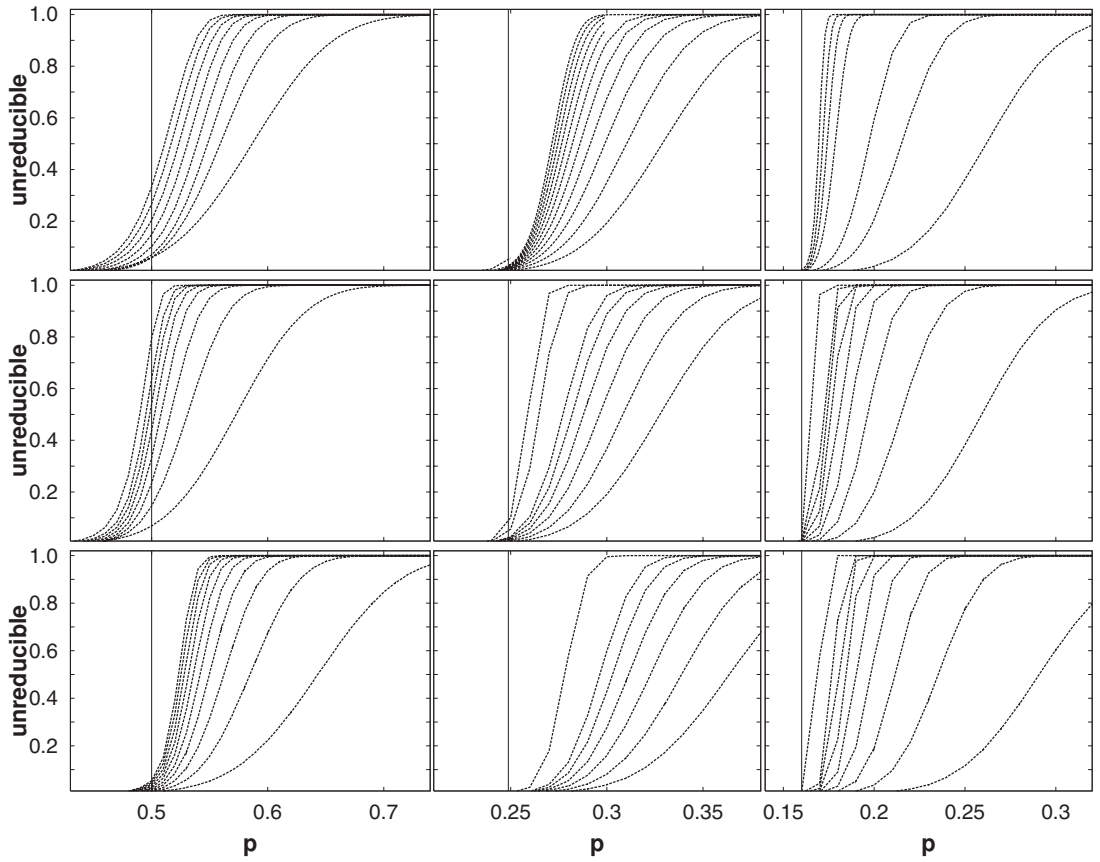

FIG. 4. Plot of the probability to obtain any nonempty remainder graph after a complete exhaustion of the reduction rules as a function of bond density p in $d=2$ (left column), $d=3$ (middle column), and $d=4$ (right column) for $\pm J$ bonds (top row), Gaussian bonds without superbond reduction SB according to rule VI (middle row), and Gaussian bonds with SB (bottom row). The sequence of graphs in each plot steepen for increasing system size L from right to left. There is a strong dependence on L, and it appears that the probabilities converge to a 0–1 step function at or near the bond-percolation threshold (indicated by a vertical line). With superbond reduction, rule VI, graphs are far more reducible even significantly above the threshold, at least at finite size.

very dependent on the recursive application of the set of rules, exhausting lower rules (which are computationally less costly) first before applying a higher rule. For instance, at least everything that is reducible by R1 and R2 could also have been reduced with SB. Thus, the further to the right a rule peaks, the more powerful it is, and its decline signals significant changes in the structure of the graph. The peak of R1 near p_c (marked by a vertical line in each plot) is a consequence of the well-known fact that a percolating graph is predominantly one connected, i.e., $p_c \sim 1/(2d)$ such that the connectivity is $\alpha_c = 2dp_c \sim 1$ for $d \to \infty$. The values for the bond-percolation thresholds on hypercubic lattices are $p_c = 1/2$ in $d=2$, $p_c \approx 0.2488$ in $d=3$, and $p_c \approx 0.1601$ in $d=4$. These thresholds are indicated by vertical lines in each plot.

The additional use of SB does not seem to affect the other rules much (except for Rd). While it does not seem to trigger avalanches of activity for lower rules (except just above p_c), it in itself often leads to nearly 10% further reduction at larger p.

In Fig. 4 we have plotted, as a function of bond density p, the fraction of instances that result in a remainder graph after a complete exhaustion of the reduction rules. We note that below and near the bond-percolation threshold p_c in each dimension, almost all graphs are completely reducible. This implies that the optimization of their energy can be done in polynomial time. Physically, this means that there cannot be an ordered, glassy state even at $T=0$ below p_c, of course. For increasing system size, a sharp transition emerges such that almost every graph has some nonempty remainder (of unspecified size) above that transition. In the case of the discrete $\pm J$ bonds, this transition appears to be related with presumed onset of spin-glass order at $p=p^* > p_c$, as discussed in Refs. 6 and 7. For Gaussian bonds, $p^*=p_c$, and the transition appears to be centered close to that. Asymptotically, the use of SB seems to push the transition just above p_c, whereas it seems to locate somewhat below without SB.

In Fig. 5 we have plotted the average size of the remainder graph (empty or not) as a function of bond density p. Including the empty remainder graphs in the weight of the average is important, of course, and explains the values below unity at low p. The pivot point indicates a well-defined transition point closely related to a three-core percolation transition[33,35,38] above p_c, as our rules reduce at least all vertices of degree less than 4. The correspondence is not exact, as cooperative effects between bond weights (such as rule III) or superbonds (rule VI) distort the pure case. Predictably, for $p \to 1$ the graphs remain unaltered, except maybe for a few spins reducible by SB at lower d.

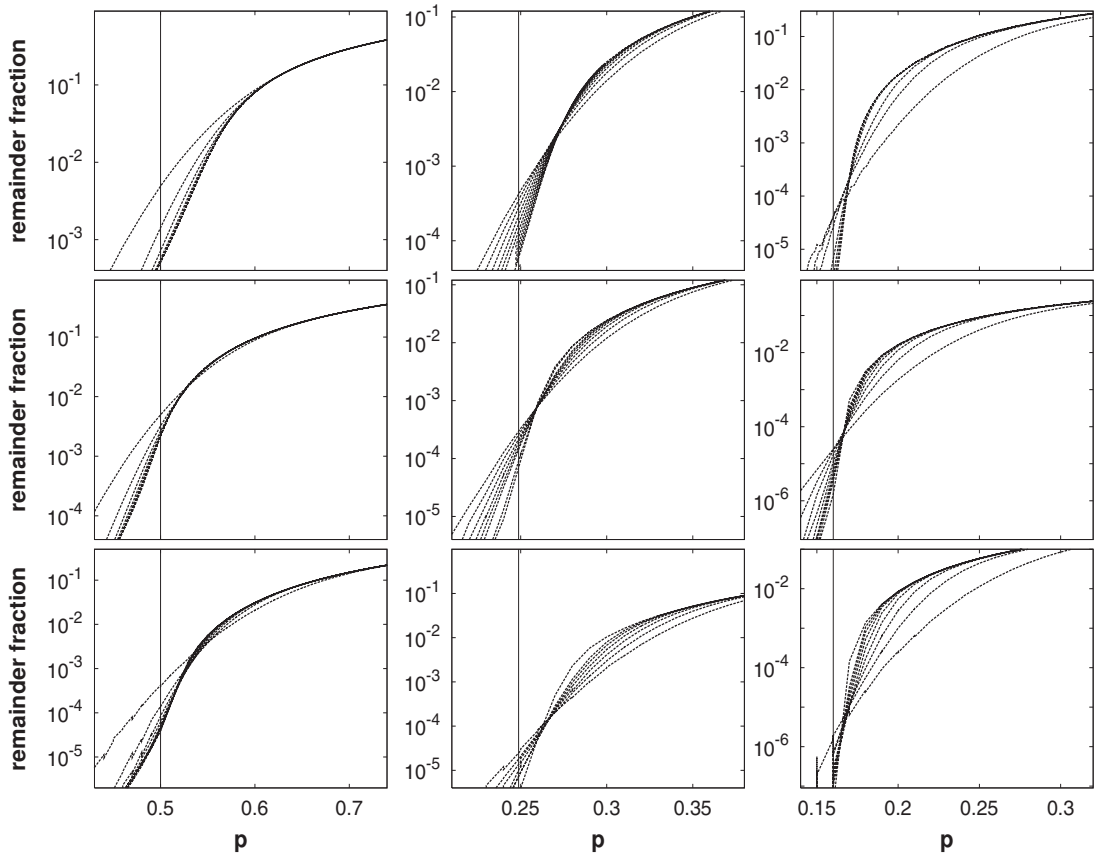

FIG. 5. Plot of the average (fractional) size of the remainder graph (empty or not) as a function of bond density p in $d=2$ (left column), $d=3$ (middle column), and $d=4$ (right column) for $\pm J$ bonds (top row), Gaussian bonds without superbond reduction SB according to Rule VI (middle row), and Gaussian bonds with SB (bottom row). Superbond reduction with rule VI lowers the remainder size near the threshold by about an order of magnitude but with diminishing effects for larger p. The sequence of graphs in each plot steepens for increasing system size L.

In Fig. 6 we have plotted the average connectivity $\langle\alpha\rangle$ of any nonempty remainder graph as a function of bond density p. By virtue of the reduction rules, it is $\langle\alpha\rangle \geq 4$. The data are very noisy below p_c since almost all remainders are empty there. These connectivities will eventually approach $2d$ for $p \to 1$, except when SB is included. There is a strong effect due to SB also right above the threshold p_c, where rule VI leads to an increasingly sharper maximum with size and dimension, as Eq. (5) is more likely satisfied there.

IV. DOMINANT BOND REDUCTION HEURISTIC

Rule VI in Sec. II is based on the following observation: If the absolute weight $|J_{i,j'}|$ of one bond incident on spin x_i from a neighboring spin $x_{j'}$ exceeds, the absolute sum of all its other $\alpha_i - 1$ bond weights with adjacent spins, i.e., if by Eq. (5)

$$r_i \equiv \sum_{j=1, j\neq j'}^{\alpha_i} \frac{|J_{i,j}|}{|J_{i,j'}|} < 1, \tag{6}$$

bond $J_{i,j'}$ *must* be satisfied in any ground state. In the exact reduction procedure, as applied in Sec. III, such a dominant bond is used to eliminate it and the spin x_i from the problem.

Here, we consider relaxing that constraint to assess the quality of approximate results that can be obtained with a heuristic approach. We assume that even if $r_i \geq 1$ in Eq. (6), any almost-dominant bond on a spin x_i is more likely satisfied in a ground state. This suggests a fast greedy heuristic: Find the spin x_i with $r_i = r_{\min} = \min_{1\leq j\leq N}\{r_j\}$ in an instance and eliminate it and its strongest bond as in rule VI. This step can be repeated until any number of the heaviest bonds has been removed to treat the remainder with an optimization heuristic like EO, or even until the *entire* lattice is reduced. The latter heuristic we call DBR.

Like rule VI itself, DBR is not useful for homogeneous bond distributions like $\pm J$, where all bonds have the same absolute weight $|J| \equiv 1$ (at least initially). However, it may be very effective for continuous bond distributions on dilute lattices with low average connectivity $\langle\alpha\rangle$, as we have shown in Sec. III. We can further exploit the universality of bond distributions and utilize *broadly distributed* bonds,[40,41] such as a power law, $P(J) \sim |J|^{-\gamma}$ for $|J| \to \infty$, as long as $P(J)$ has zero mean and finite width. In fact, such a greedy procedure has already been described for extremely widely separated bonds (each bond is larger in weight that the sum of *all* smaller ones), where it becomes exact:[42,43] the problem is no longer NP hard. For the power-law bonds, we expect that there is a transition in the behavior of this procedure at some finite

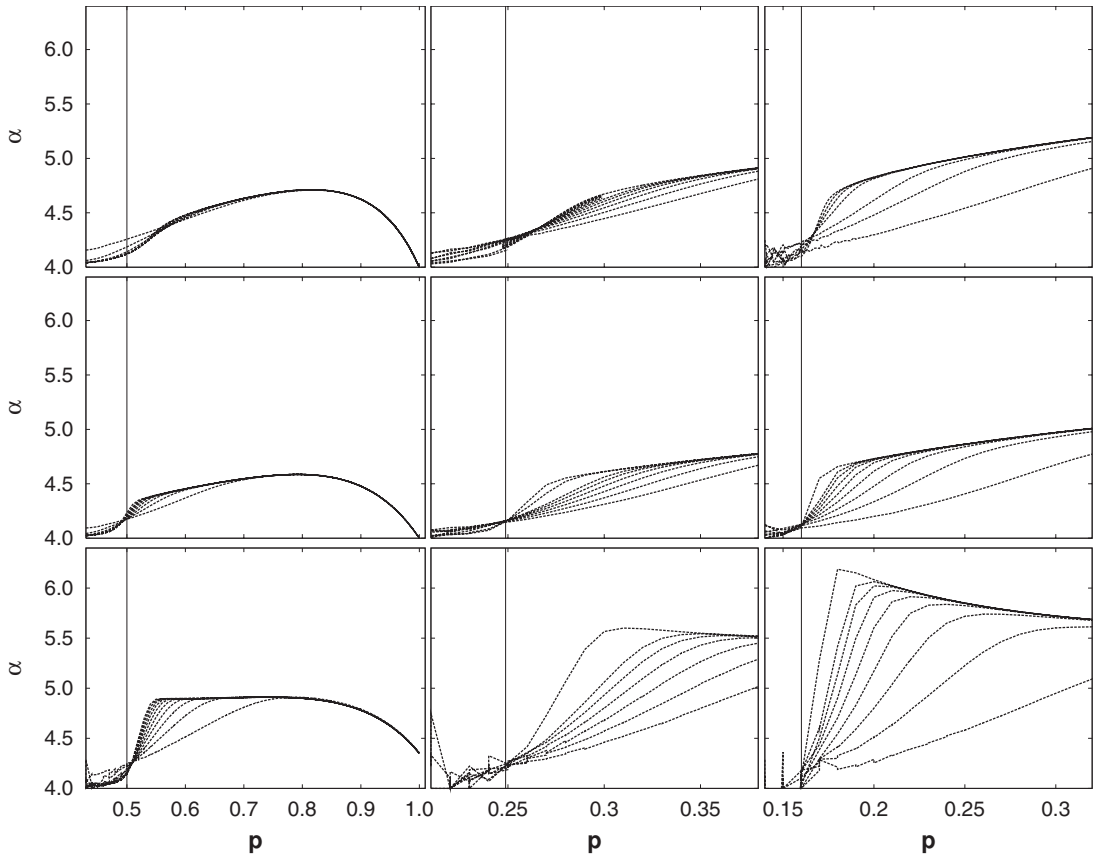

FIG. 6. Plot of the average connectivity $\langle\alpha\rangle$ of any nonempty remainder graph as a function of bond density p in $d=2$ (left column), $d=3$ (middle column), and $d=4$ (right column) for $\pm J$ bonds (top row), Gaussian bonds without superbond reduction SB according to rule VI (middle row), and Gaussian bonds with SB (bottom row). The dramatic effect of implementing rule VI becomes apparent near the percolation threshold, especially for increasing d. The sequence of graphs in each plot steepens for increasing system size L.

value of γ_c. Hence, we may find a "sweet spot:" a sufficiently broad distribution on a sufficiently dilute lattice for efficient DBR on very large lattices, while p just above p_c and γ just above γ_c ensure the EA universality class in any dimension.

Frustration leaves many bonds violated in the ground state, obviously, and our recursive elimination procedure accounts for that through compounding bonds in rule III, as described also in Fig. 2. In a simple benchmark, shown in Fig. 7, we found that DBR obtains an approximate ground-state energy density of $\langle e\rangle_N=-1.308(1)$ for the undiluted EA, in $d=2$ at $N=100^2$, only 0.5% above $\langle e\rangle_\infty=-1.314\ 79(2)$, the best-known result,[39] and in $d=3$ at $N=20^3$, 4% above $\langle e\rangle_\infty=-1.700(1)$.[44] Computational costs are trivial, $O(dN\ln N)$, but our implementation is limited to $N<10^4$ by a data structure problem: repeated application of rule VI leads to a few highly connected spins with hundreds of neighbors. Of course, to calculate properties of low-T excitations, even a systematic error of 4% would be unacceptably large, and our naive DBR algorithm will have to be developed into a metaheuristic, again combining reduction and EO.

To explore the effect of broadly distributed bonds, we have compared DBR for one undiluted cubic lattice of size $N=20^3$ with Gaussian and power-law bonds at $\gamma=1.5$. In Fig. 8, we show the value of the (smallest) $r_i=r_{\min}$ in Eq. (6) of the currently reduced spin x_i during one run of DBR. Initially, for all $r_{\min}<1$, DBR is exact, which persists much longer for power-law bonds. Even when $r_{\min}\geq 1$, the value of $r_{\min}$ is typically smaller for power-law bonds. Considering that DBR's systematic error is only 4% for Gaussian bonds, we project that power-law bonds should be even more successful. We expect to conduct more extensive tests for varying γ and increasing N, which will require a significantly revised data structure compared to the one used in these studies.

V. CONCLUSIONS

Our results validate the effectiveness of the recently proposed reduction scheme to determine the stiffness exponent y,[8] leaving remainder graphs that are a small fraction (typically $\approx 1-10\%$) of the size of the original problem in the interesting regime just above p_c. Note that the fact that reduction works well in two-dimensions, where $T_c=0$ holds, does not imply definitively that it should work for $d>2$. Nevertheless, since the local interconnections between spins (i.e., graph vertices) near and just above p_c in $d=2$ and higher dimensions are similar, it justifies that the reduction scheme is applicable also for higher dimensions,[6,7,24] or even sparse random graphs,[31,32] where no exact ground-state algorithms are available. As the general discussion and the speculative inferences in the Appendix suggest, it may be possible

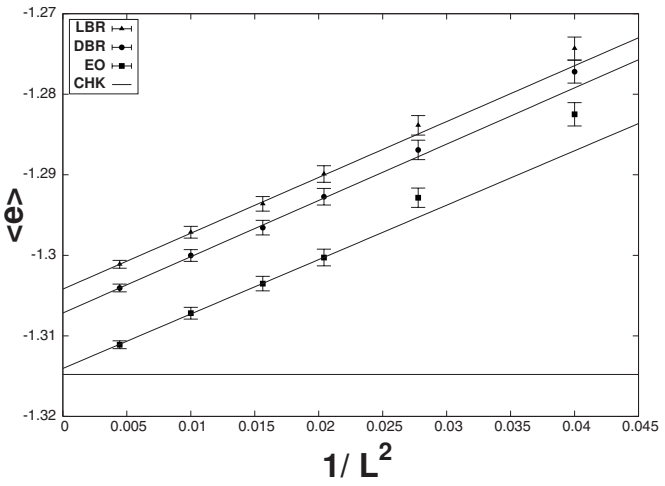

FIG. 7. Extrapolation plot of approximate ground-state energy densities $\langle e\rangle = \langle E\rangle / L^2$ for the two-dimensional EA in Eq. (1) as a function of $1/L^2$. Each data point is the average over 10^4 random instances. The results for the DBR heuristic (circles) discussed in the text extrapolate to within 0.5% of the best-known prediction by Campbell-Hartmann-Katzgraber (CHK) (Ref. 39) marked by the horizontal line. Shown are also results obtained with the EO heuristic (squares) (Refs. 22 and 23), which reproduces CHK within errors, and a simple alternative to DBR we call least bond reduction (LBR, triangles). LBR also applies rule VI but to the spin with the weakest total bond-weight, i.e., where the sum of all absolute weights of incident bonds is minimal. Both, DBR and LBR, are much faster than EO. LBR is marginally simpler than DBR and avoids the creation of highly connected spins.

to extend the methods discussed here for any particular graph topology or bond distribution at hand. We have also presented evidence that a heuristic approach, based purely on the bond reductions introduced in Sec. II, provides a fast algorithm to obtain approximate ground states, with the potential to handle even large or undiluted systems within bounded error.

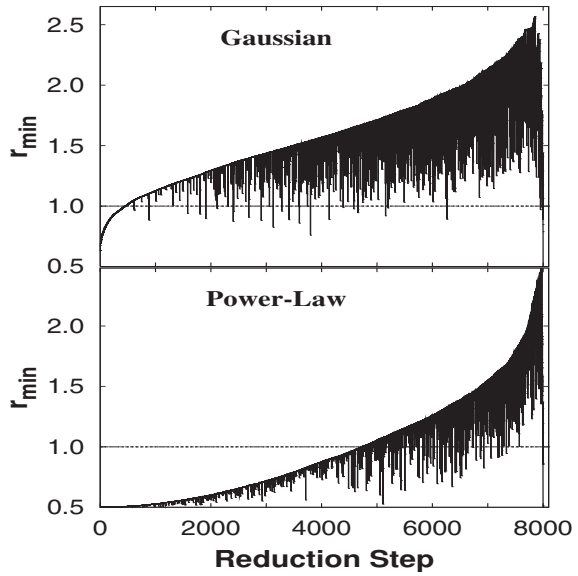

FIG. 8. Plot of $r_{\min}$ during a run of DBR on a $N=20^3$ lattice with Gaussian (top) and power-law bonds at $\gamma=1.5$ (bottom).

ACKNOWLEDGMENTS

S.B. thanks P. Duxbury for inspiring discussions. This work was supported by Grant No. 0312510 from the Division of Materials Research at the National Science Foundation and a grant from the Emory University Research Council.

APPENDIX

In general, a spin-glass Hamiltonian H, such as the one in Eq. (1), consists of the sum (in the negative) of a number of terms $J_{i_1,\ldots,i_p} x_{i_1} \ldots x_{i_p}$, each representing a (hyper)bond of weight J between p spins $x_i \in \{-1,+1\}$. The number of connected spins p may vary between terms, although $p=2$ for all terms in Eq. (1). The bonds J are quenched variables drawn from an arbitrary distribution, discrete or continuous. A particular *instance* of the spin-glass Hamiltonian is specified by the values of these quenched variables.

A ground state minimizes H, thus we want to maximize as many terms as possible in $-H$. Each spin, say, x_0, appears in a number of such terms, connecting it to a total of q other spins. In general, there are 2^q possible terms, and we can *eliminate* $x_0 = \pm 1$ by

$$\begin{aligned} & J_0 x_0 + J_1 x_1 x_0 + \ \ldots\ + J_q x_q x_0 + J_{12} x_1 x_2 x_0 + \ \ldots \\ & \quad + J_{1\ldots q} x_1 \ldots x_q x_0 \\ & = x_0 (J_0 + J_1 x_1 + \ \ldots\ + J_q x_q + J_{12} x_1 x_2 \\ & \quad + \ \ldots\ + J_{1\ldots q} x_1 \ldots x_q) \\ & \le |J_0 + J_1 x_1 + \ \ldots\ + J_q x_q + J_{12} x_1 x_2 \\ & \quad + \ \ldots\ + J_{1\ldots q} x_1 \ldots x_q| \\ & = a_0 + a_1 x_1 + \ \ldots\ + a_q x_q + a_{12} x_1 x_2 \\ & \quad + \ \ldots\ + a_{1\ldots q} x_1 \ldots x_q, \end{aligned} \tag{A1}$$

where the bound again becomes an equality for the ground-state energy. A new Hamiltonian is obtained which is reduced by one variable. Notice that the last two lines provide a unique system of 2^q linear equations, one for each assignment of the $x_i = \pm 1$, which determine the new bonds a in terms of the old bonds J.

To solve the linear system, we define

$$g(\mathbf{x}) = |J_0 + J_1 x_1 + \ \ldots\ + J_q x_q + J_{12} x_1 x_2 + \ \ldots\ + J_{1\ldots q} x_1 \ldots x_q|, \tag{A2}$$

and note that for *any* function $g(\mathrm{x})$, $\mathbf{x} \in \{\pm 1\}^q$, it is true that

$$\begin{aligned} g(\mathbf{x}) &= \sum_{\{\epsilon\}} g(\epsilon) \prod_{i=1}^{q} \delta_{x_i,\epsilon_i} \\ &= \sum_{\{\epsilon\}} g(\epsilon) \prod_{i=1}^{q} \frac{1+\epsilon_i x_i}{2} \\ &= \sum_{\{\epsilon\}} \frac{g(\epsilon)}{2^q} (1 + \epsilon_1 x_1 + \ \ldots\ + \epsilon_q x_q + \epsilon_1 \epsilon_2 x_1 x_2 + \ \ldots \\ &\quad + \epsilon_{q-1} \epsilon_q x_{q-1} x_q + \ \ldots\ + \epsilon_1 \ldots \epsilon_q x_1 \ldots x_q), \end{aligned} \tag{A3}$$

where the sum extends over all 2^q permutations of $\epsilon \in \{\pm 1\}^q$ and the relation $\delta_{a,b}=(1+ab)/2$ for $a,b \in \{\pm 1\}$ was used to represent the Kronecker symbol. Comparison of Eq. (A3) with the last two lines in Eq. (A1) yields

$$a_{i_1,\ldots,i_p} = \frac{1}{2^q}\sum_{\{\epsilon\}} g(\epsilon)\epsilon_{i_1}\ldots\epsilon_{i_p} \tag{A4}$$

for the new bonds connecting the remaining variables.

In general, it is not useful to reduce the Hamiltonian in this way; after all, if all n spins are connected to each other, as for the Sherrington-Kirkpatrick model,[45] just the elimination of *one* spin-variable requires $O(2^n)$ operations. Yet, there are common situations, in particular, for lattices of finite dimensionality and sparse graphs, where the application of the previous results can be very useful: either in itself, in combination with heuristic techniques, or as the basis of approximation schemes. Of course, we may also be interested in the system's entropy, the magnetization, overlaps, etc., which can be considered simultaneously.[8]

Although the combinatorial effort in the preceding expressions seems daunting in general, they possess a rich structure that relates them to other, well-studied subjects. For instance, we can rewrite Eq. (A4) as

$$a_{i_1,\ldots,i_p} = \frac{1}{2^q}\sum_{j=0}^{2^q-1} g(\{j\})W_{k,2^q}(j), \tag{A5}$$

with

$$k = 1 + \sum_{\mu=1}^{p} 2^{i_\mu - 1}, \tag{A6}$$

where $\{j\}$ is the binary encoding (on ± 1) of the integer j. In particular, $W_{k,L}(x)$ is the kth Walsh function[46] of support L familiar from wavelet analysis and signal filtering. The orthogonality properties of Walsh functions provide a powerful means to analyze the preceding reduction equations for particular choices of initial bond distributions. For instance, there may be types of graphs with a nontrivial bond distribution for which the reductions could be simple. Also, a transformation may be found that maps the distribution of J's into that of a's. Finally, the existing highly optimized wavelet algorithms[47] may in fact produce efficient spin-glass solvers based on these reduction equations.

*www.physics.emory.edu/faculty/boettcher/
†www.physics.emory.edu/students/davidheiser/

[1] K. Binder and A. P. Young, Rev. Mod. Phys. **58**, 801 (1986).
[2] M. Mézard, G. Parisi, and M. A. Virasoro, *Spin Glass Theory and Beyond* (World Scientific, Singapore, 1987).
[3] K. H. Fischer and J. A. Hertz, *Spin Glasses* (Cambridge University Press, Cambridge, 1991).
[4] *Spin Glasses and Random Fields*, edited by A. P. Young (World Scientific, Singapore, 1998).
[5] S. F. Edwards and P. W. Anderson, J. Phys. F: Met. Phys. **5**, 965 (1975).
[6] S. Boettcher, Europhys. Lett. **67**, 453 (2004).
[7] S. Boettcher, Eur. Phys. J. B **38**, 83 (2004).
[8] S. Boettcher, Eur. Phys. J. B **33**, 439 (2003).
[9] S. Boettcher and E. Marchetti, Phys. Rev. B **77**, 100405(R) (2008).
[10] M. J. Stephen and G. S. Grest, Phys. Rev. Lett. **38**, 567 (1977).
[11] B. W. Southern, A. P. Young, and P. Pfeuty, J. Phys. C **12**, 683 (1979).
[12] A. J. Kolan and R. G. Palmer, J. Appl. Phys. **53**, 2198 (1982).
[13] J. R. Banavar, A. J. Bray, and S. Feng, Phys. Rev. Lett. **58**, 1463 (1987).
[14] A. J. Bray and S. Feng, Phys. Rev. B **36**, 8456 (1987).
[15] A. Coniglio, Phys. Rev. Lett. **62**, 3054 (1989).
[16] A. Coniglio, Physica A **266**, 379 (1999).
[17] C. M. Fortuin and P. W. Kasteleyn, Physica (Amsterdam) **57**, 536 (1972).
[18] V. Cataudella, G. Franzese, M. Nicodemi, A. Scala, and A. Coniglio, Phys. Rev. E **54**, 175 (1996).
[19] A. Fierro, G. Franzese, A. de Candia, and A. Coniglio, Phys. Rev. E **59**, 60 (1999).
[20] G. Franzese and A. Coniglio, Phys. Rev. E **59**, 6409 (1999).
[21] T. Jörg and F. Ricci-Tersenghi, Phys. Rev. Lett. **100**, 177203 (2008).
[22] S. Boettcher and A. G. Percus, Phys. Rev. Lett. **86**, 5211 (2001).
[23] S. Boettcher and A. G. Percus, Artif. Intell. **119**, 275 (2000).
[24] S. Boettcher, Phys. Rev. Lett. **95**, 197205 (2005).
[25] T. Aspelmeier, M. A. Moore, and A. P. Young, Phys. Rev. Lett. **90**, 127202 (2003).
[26] G. Parisi and T. Rizzo, arXiv:0706.1180 (unpublished).
[27] T. Aspelmeier, A. Billoire, E. Marinari, and M. A. Moore, arXiv:0711.3445 (unpublished).
[28] T. Jörg, Proceedings of the Statistical Physics of Disordered Systems and Its Applications, Hayama, Japan, 2004 (unpublished).
[29] T. Jörg, Phys. Rev. B **73**, 224431 (2006).
[30] M. Hasenbusch, A. Pelissetto, and E. Vicari, J. Stat. Mech.: Theory Exp. (2008) L02001.
[31] S. Boettcher, Eur. Phys. J. B **31**, 29 (2003).
[32] S. Boettcher, Phys. Rev. B **67**, 060403(R) (2003).
[33] C. Farrow, P. M. Duxbury, and C. F. Moukarzel, Phys. Rev. E **72**, 066109 (2005).
[34] J. I. Alvarez-Hamelin, L. Dall'Asta, A. Barrat, and A. Vespignani, Adv. Neural Inf. Process. Syst. **18**, 41 (2006).
[35] C. L. Farrow, P. Shukla, and P. M. Duxbury, J. Phys. A: Math. Theor. **40**, F581 (2007).
[36] D. J. Frank and C. J. Lobb, Phys. Rev. B **37**, 302 (1988).
[37] D. B. Gingold and C. J. Lobb, Phys. Rev. B **42**, 8220 (1990).
[38] J. Adler, Physica A **171**, 453 (1991).
[39] I. A. Campbell, A. K. Hartmann, and H. G. Katzgraber, Phys. Rev. B **70**, 054429 (2004).
[40] P. Cizeau and J. P. Bouchaud, J. Phys. A **26**, L187 (1993).
[41] K. Janzen, A. K. Hartmann, and A. Engel, J. Stat. Mech.: Theory Exp. (2008) P04006.
[42] C. M. Newman and D. L. Stein, Phys. Rev. Lett. **72**, 2286

(1994).
[43] M. Cieplak, A. Maritan, and J. R. Banavar, Phys. Rev. Lett. **72**, 2320 (1994).
[44] K. F. Pal, Physica A **233**, 60 (1996).
[45] D. Sherrington and S. Kirkpatrick, Phys. Rev. Lett. **35**, 1792 (1975).
[46] M. Thuillard, *Wavelets in Soft Computing* (World Scientific, Singapore, 2001).
[47] G. Beylkin, R. Coifman, and V. Rokhlin, Commun. Pure Appl. Math. **44**, 141 (1991).